

This is the accepted manuscript made available via CHORUS. The article has been published as:

$\beta$ -decay half-lives of  $^{134,134m}\text{Sb}$  and their isomeric yield ratio produced by the spontaneous fission of  $^{252}\text{Cf}$

K. Siegl, K. Kolos, N. D. Scielzo, A. Aprahamian, G. Savard, M. T. Burkey, M. P. Carpenter, P. Chowdhury, J. A. Clark, P. Copp, G. J. Lane, C. J. Lister, S. T. Marley, E. A. McCutchan, A. J. Mitchell, J. Rohrer, M. L. Smith, and S. Zhu

Phys. Rev. C **98**, 054307 — Published 14 November 2018

DOI: [10.1103/PhysRevC.98.054307](https://doi.org/10.1103/PhysRevC.98.054307)

# $\beta$ -decay half-lives of $^{134,134m}\text{Sb}$ and their isomeric yield ratio produced by the spontaneous fission of $^{252}\text{Cf}$

K. Siegl,<sup>1,2</sup> K. Kolos,<sup>2</sup> N. D. Scielzo,<sup>2</sup> A. Aprahamian,<sup>1</sup> G. Savard,<sup>3,4</sup> M. T. Burkey,<sup>3,4</sup>  
M. P. Carpenter,<sup>4</sup> P. Chowdhury,<sup>5</sup> J. A. Clark,<sup>4</sup> P. Copp,<sup>5</sup> G. J. Lane,<sup>6</sup> C. J. Lister,<sup>5</sup>  
S. T. Marley,<sup>7</sup> E. A. McCutchan,<sup>8</sup> A. J. Mitchell,<sup>5,6</sup> J. Rohrer,<sup>4</sup> M. L. Smith,<sup>6</sup> and S. Zhu<sup>4</sup>

<sup>1</sup>*Department of Physics, University of Notre Dame, Notre Dame, Indiana 46556, USA*

<sup>2</sup>*Nuclear and Chemical Sciences Division, Lawrence Livermore National Laboratory, Livermore, California 94550, USA*

<sup>3</sup>*Department of Physics, University of Chicago, Chicago, Illinois 60637, USA*

<sup>4</sup>*Physics Division, Argonne National Laboratory, Argonne, Illinois 60439, USA*

<sup>5</sup>*Department of Physics and Applied Physics, University of Massachusetts Lowell, Lowell, MA 01854, USA*

<sup>6</sup>*Department of Nuclear Physics, Research School of Physics and Engineering,  
The Australian National University, Canberra, ACT 2601, Australia*

<sup>7</sup>*Department of Physics and Astronomy, Louisiana State University, Baton Rouge, LA 70803, USA*

<sup>8</sup>*Brookhaven National Laboratory, National Nuclear Data Center, Upton, NY 11973 USA*

(Dated: October 16, 2018)

A number of fission products possess isomeric states which have a nuclear spin significantly different from that of the ground state. The yield ratio of these states following fission is influenced by the angular momentum present in the fissioning system. The  $^{134m,134}\text{Sb}$  yield ratio had not been previously measured in the spontaneous fission of  $^{252}\text{Cf}$ ; however, it had previously been observed to favor the  $(7^-)$  isomer over the  $(0^-)$  ground state in  $^{235}\text{U}(\text{n}_{\text{th}},\text{f})$  and  $^{232}\text{Th}(25\text{ MeV p},\text{f})$ . Using a mass-separated beam of low-energy  $^{134,134m}\text{Sb}$  ions produced by  $^{252}\text{Cf}$  spontaneous fission at the CARIBU facility,  $\beta$  particles and  $\gamma$  rays were detected using the SATURN/X-Array decay station to determine the fission-yield ratio and  $\beta$ -decay half-lives. The  $^{134m}\text{Sb}$  to  $^{134}\text{Sb}$  fission yield was determined to be  $2.03 \pm 0.05$  and the half-lives of  $^{134m}\text{Sb}$  and  $^{134}\text{Sb}$  were found to be  $9.87 \pm 0.08\text{ s}$  and  $0.674 \pm 0.004\text{ s}$ , respectively. These results represent the first isomeric yield ratio measurement for this nucleus, and improved measurements of the  $^{134}\text{Sb}$  ground-state and the  $^{134m}\text{Sb}$  isomer half-lives.

## I. INTRODUCTION

In nuclear fission, an atomic nucleus separates into two fragments, which rapidly deexcite through the emission of prompt neutrons and  $\gamma$  rays. The resulting nuclei, referred to as fission products, are produced in both the ground state and isomeric states, with the long-lived isomeric states typically arising from a small difference in mass from the ground state, a large difference in intrinsic angular momentum, or both. The ratio of isomeric to ground state independent fission yields, referred to here simply as the isomeric yield ratio, is an observable which can be used to infer the initial spin distribution in the primary fission fragments [1].

Isomeric yield ratios are important for understanding the development of radiation released after fission. The fission-product ground and isomeric states often have significantly different  $\beta$ -decay properties such as half-lives,  $\gamma$ -ray and delayed-neutron emission properties, and lepton energy distributions [2]. Therefore, isomeric yield ratios provide critical input parameters to decay-heat calculations for nuclear reactors, and for addressing the reactor antineutrino anomaly [3].

Previous measurements of isomeric yield ratios have generally used either Isotope Separation Online (ISOL) approaches [4, 5] or chemical-separation methods. The ISOL approach is limited to high energy fission, most commonly charged-particle-induced fission, and has been performed on several actinides to determine the isomeric yield ratio for several nuclei. The energy and species

of the charged particle used to induce fission determine the amount of angular momentum added to the system. The effect of these parameters on the isomeric yield ratio has previously been studied [11] and consistently showed that an increase in conferred angular momentum leads to increased yield of the high-angular-momentum state relative to the low-angular-momentum state. This technique, however, is limited to only non-refractory chemical species.

Previous measurements of spontaneous and thermal-neutron-induced fission were only possible by chemical-separation processes applied to fission products accumulated on foils. However, the deposition and chemical-separation is often slower than the lifetimes of the shorter-lived isobars so it was necessary to account for the feeding into and decay out of the species of interest to extract isomeric yield ratios, resulting in large uncertainties [6–10].

In all previous measurements focused on determining the isomeric yield ratios,  $\gamma$ -ray spectroscopy was used to identify the isomeric and ground state decays, and therefore measurements were limited to cases where both have well-characterized  $\gamma$  rays of sufficient intensity. Although this allowed measurements to be made even in the presence of other decaying isotopes, it introduced additional uncertainty from the absolute intensities of the  $\gamma$ -ray transitions.

The Californium Rare Isotope Breeder Upgrade (CARIBU) facility at Argonne National Laboratory (ANL) can deliver pure beams of mass-separated ions

from spontaneous fission with extraction significantly faster than chemical separation. In this work,  $^{134,134m}\text{Sb}$  was delivered to the experiment with an average preparation time of  $80 \pm 15$  ms. The isomeric yield ratio is determined without relying directly on the absolute intensities of characteristic  $\gamma$  rays. As only the nuclear species of interest is present in the beam, the isomeric yield ratio could be determined from the build-up and decay of the  $\beta$ -particle signal.

In order to interpret the time dependence of the  $\beta$ -particle count rate, precision measurements of the half-lives of the two species were necessary. The  $\beta$  decay of  $^{134m}\text{Sb}$ , the 279-keV excitation isomer [12], produces multiple high-intensity  $\gamma$  rays, which allows a straightforward way to determine the half-life through  $\gamma$ -ray spectroscopy. However, the  $\beta$  decay of  $^{134}\text{Sb}$  is dominated by the  $0^-$  to  $0^+$  transition to the ground state of  $^{134}\text{Te}$  [15, 16] and does not have any high-intensity  $\gamma$  rays. Therefore, the  $^{134}\text{Sb}$  half-life was determined from the  $\beta$ -particle decay curve. Once the half-lives were determined to high precision, these values were used in the determination of the isomeric yield ratio from the  $\beta$ -particle counting.

The only previous isomer-yield-ratio estimates for  $^{134,134m}\text{Sb}$  were in  $^{235}\text{U}$  thermal neutron induced fission [13] and  $^{232}\text{Th}$  25-MeV proton induced fission [14]. Both cases showed a favored production of  $^{134m}\text{Sb}$  although the isomeric yield ratio was not well quantified.

## II. EXPERIMENTAL TECHNIQUES

The ( $J^\pi = (0^-)$ )  $^{134}\text{Sb}$  and ( $J^\pi = (7^-)$ )  $^{134m}\text{Sb}$  ions were produced from the spontaneous fission of a  $\sim 1.7\text{-Ci}$   $^{252}\text{Cf}$  source at the CARIBU facility. The  $^{252}\text{Cf}$  fission fragments were thermalized using a large helium-filled gas catcher and extracted as a continuous low-energy beam of singly-charged ions from the nozzle of this device using a combination of gas flow and electric fields [17, 18]. The beam was sent through an isobar separator [19] operated with a mass resolution of  $\frac{M}{\Delta M} \approx 15000$  to isolate  $^{134,134m}\text{Sb}$ . A radiofrequency quadrupole (RFQ) buncher containing residual helium gas was used to accumulate, cool, and bunch the beam with a timing of 100 ms between bunches [17]. The ion bunches were delivered through an electrostatic beam line to a decay station with an intensity of  $\sim 400$  ions per second.

The decay station consisted of the Scintillator And Tape Using Radioactive Nuclei (SATURN) surrounded by an array of five high-purity Germanium (HPGe) clover detectors (X-Array), described in detail in Ref. [20]. For this experiment SATURN used a cylindrical ‘well’ plastic-scintillator  $\beta$  detector, a 10-cm diameter cylinder 10 cm in length. The detector has a 6-mm diameter well bored in it to allow the beam to implant on a 35-mm-wide aluminized-mylar tape which passes through a slot in the middle of the detector oriented at  $90^\circ$  to the beam direction. The collection point on the tape is positioned

to be at the geometric center of the HPGe  $\gamma$  detector array. Energy and efficiency calibrations for SATURN and the X-Array were determined using standard calibrated  $\beta$  and  $\gamma$ -ray spectroscopy sources. The plastic scintillator was operated with a  $\beta$ -particle energy threshold of  $500 \pm 200$  keV, resulting in an  $\approx 97\%$  detection efficiency for the decays of  $^{134,134m}\text{Sb}$  which release over 8 MeV of energy. The purpose of the movable tape was to limit contributions from the  $\beta$ -decay products  $^{134}\text{Te}$  ( $t_{1/2}=41.8$  min) and  $^{134}\text{I}$  ( $t_{1/2}=52.5$  min). The majority of the data were acquired with the bunched beam implanted for 2.5 s, after which it was deflected from the beam line for 2.5 s. The tape was then moved, and after an additional 1.5 s (providing time to assess any remaining backgrounds) the beam was returned to the tape. This is subsequently referred to as the “short tape cycle.” Data were also acquired with a “long tape cycle” consisting of 30 s of implantation, 30 s of decay, and 16 s to assess backgrounds after the tape was moved. In the short tape cycle the time dependence of the total  $\beta$ -decay rate was primarily sensitive to the half-life of  $^{134}\text{Sb}$ , while the long tape cycle was better suited to study the long-lived  $^{134m}\text{Sb}$  decay.

The data acquisition recorded the time and energy associated with each detector trigger and coincidences were identified for events which occurred within a  $2\text{ }\mu\text{s}$  window. The  $\beta$ - $\gamma$  coincidence of the characteristic  $\gamma$  rays of  $^{134m}\text{Sb}$  in the long tape cycle were used to determine the half-life of the isomeric state. Using this half-life result, the isomeric yield ratio as well as the  $^{134}\text{Sb}$  half-life were determined from the build up and decay of the  $\beta$ -decay rate during the short tape cycle. An independent non-paralyzing dead-time of  $4.5\text{ }\mu\text{s}$  was found for each channel of the data acquisition, and a rate-dependent correction was applied to the time dependence of the  $\beta$ -singles and  $\beta$ - $\gamma$  coincidences.

## III. RESULTS AND DISCUSSION

### A. $^{134m}\text{Sb}$ half-life

The decay of  $^{134m}\text{Sb}$  primarily populates the 2398- and 1691-keV levels of  $^{134}\text{Te}$ , resulting in the emission of  $297.0 \pm 0.1$ -,  $706.3 \pm 0.1$ -, and  $1279.1 \pm 0.1$ -keV  $\gamma$  rays with intensities of  $97 \pm 5\%$ ,  $57 \pm 3\%$ , and  $100 \pm 5\%$  respectively [13]. The  $\beta$ -gated  $\gamma$ -ray spectrum detected using the long tape cycle are shown in Fig. 1.

Fits to the build up and decay of each  $\beta$ -gated  $\gamma$ -ray, shown in Fig. 2, were used to determine the half-life of  $^{134m}\text{Sb}$ . A gradual increase in  $^{134}\text{Te}$  and  $^{134}\text{I}$   $\gamma$  rays in the coincidence spectrum was observed over the course of the experiment. This background was consistent with  $(7 \pm 3)\%$  of the delivered beam being implanted in the  $\beta$  detector and not transported away during tape moves. The inclusion of this residual activity contributed a  $(0.6 \pm 0.3)\%$  shift in the determination of the  $^{134m}\text{Sb}$  half-life. The 1279-keV  $\gamma$ -ray coincidence was corrected

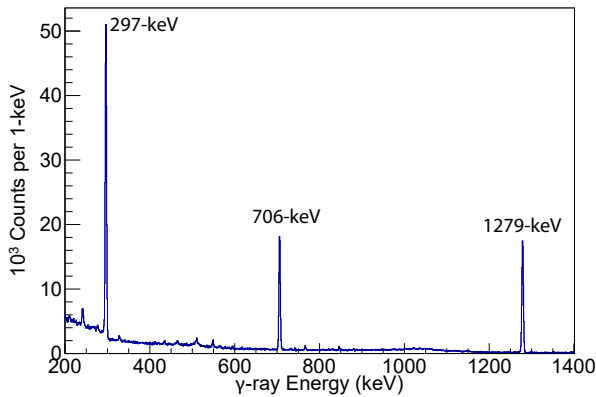


FIG. 1: The  $\gamma$ -ray energy spectrum, with constant background lines subtracted, of the  $\beta$ -gated  $\gamma$ -ray coincidences in the long tape cycle with the 297-, 706-, and 1279-keV  $\gamma$  rays.

for the presence of the  $\gamma$ -ray in the decay of  $^{134}\text{Sb}$  at an intensity of 1.1(5)% by the inclusion of a 0.50(25)% contribution to the fit of the line with the  $^{134}\text{Sb}$  half-life. The systematic uncertainty for the half-life determined by each  $\gamma$  ray includes the sensitivity of the result to the selection of the coincidence-timing window, the dead time, the presence of backgrounds, and the activity implanted in the detector. The three  $\beta$ -gated  $\gamma$ -ray results, shown in Table I, agreed well within uncertainty resulting in an average half-life of  $9.87 \pm 0.04 \pm 0.07$  s (at  $1\sigma$ ) for  $^{134m}\text{Sb}$ , where the first uncertainty is statistical and the second systematic. The value presented here is lower than the currently-adopted value of  $10.07 \pm 0.05$  s [21] by  $2\sigma$ ; it is also lower than the previous results of  $10.3 \pm 0.5$  s [13],  $10.2 \pm 0.3$  s [22], and  $10.3 \pm 0.4$  s [23],  $11.1 \pm 0.8$  s [24], although these other results have significantly larger uncertainties.

### B. $^{134}\text{Sb}$ half-life

In order to determine the half-life of  $^{134}\text{Sb}$ , the  $\beta$  singles for the short tape cycle were used. The time dependence of the detected  $\beta$ -decay rate was fit to a model which included  $^{134}, ^{134m}\text{Sb}$  as well as the decay product  $^{134}\text{Te}$ , and the time structure of the bunched beam. The results are shown in Fig. 3a. The half-life of  $^{134m}\text{Sb}$  was fixed to the value determined in the previous subsection.

The  $^{134}\text{Sb}$  half-life was determined to be  $0.6744 \pm 0.0034 \pm 0.0019$  s, which is lower and approximately an order of magnitude more precise than the previous evaluated average of  $0.78 \pm 0.06$  s [15], that is a weighted average of two measurements. In the previous works, a half-life of  $0.75 \pm 0.07$  s was determined from the time dependence of the low-intensity  $\gamma$  rays following the decay of  $^{134}\text{Sb}$  [25] and a half-life of  $0.85 \pm 0.10$  s was determined from analysis of the build up and decay of the  $\beta$  radiation with energy exceeding

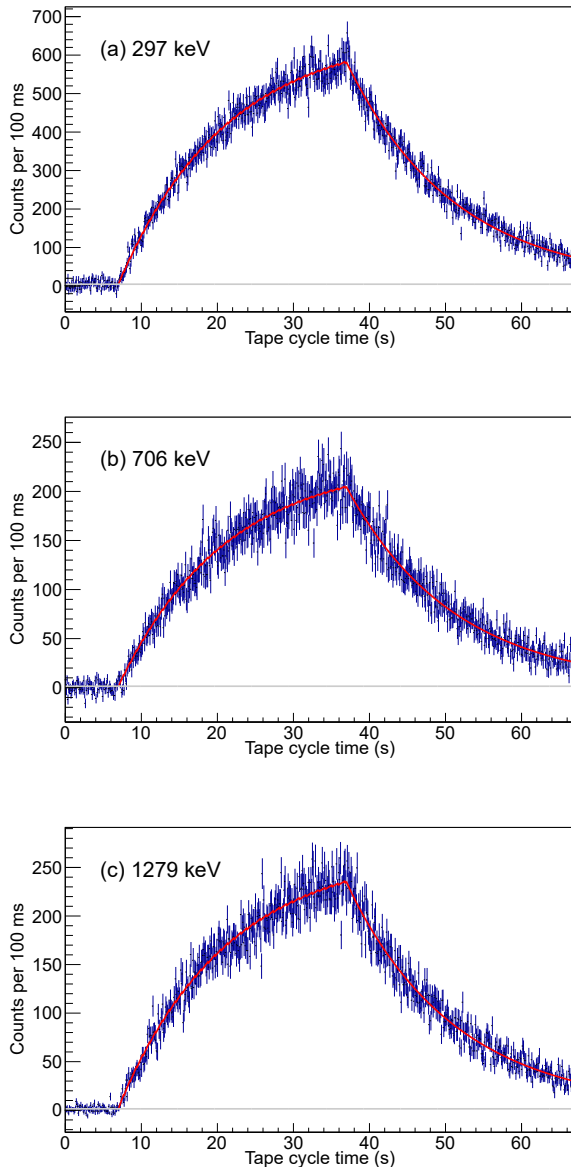


FIG. 2: (Color Online) The time dependence of the build up and decay of the  $\beta$ -gated  $\gamma$  counts during the long tape cycle for a) 297-keV, b) 706-keV, and c) 1279-keV  $\gamma$  rays.

that available to the leptons in the  $^{134m}\text{Sb}$  decay [13].

### C. Isomeric yield ratio

The isomeric yield ratio is stated as the ratio of the yield of the high-spin to low-spin nuclear states,  $\sigma_h/\sigma_l$ . The observed ratio of  $^{134m}\text{Sb}$  to  $^{134}\text{Sb}$  was determined from consistent results obtained from the  $\beta$  singles build-up and decay for both the short and long tape cycles shown in Fig. 3 after taking into account the relative efficiency for  $\beta$  detection for each species, as well as the decay losses incurred during the transport time to the

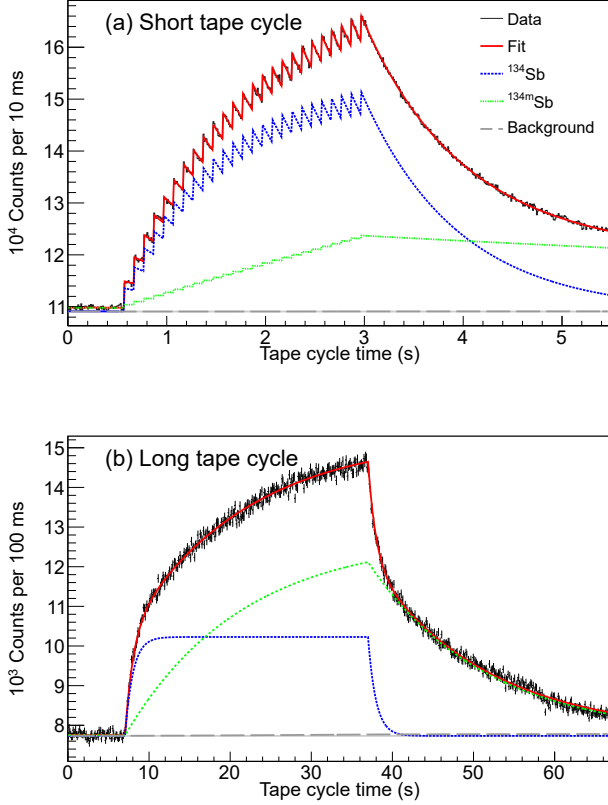


FIG. 3: (Color Online) The  $\beta$ -singles counts collected during the (a) short and (b) long tape-cycle time (black) compared to fit results (red solid line) which include contributions from the decays of  $^{134}\text{Sb}$  (blue or dark dashed line),  $^{134m}\text{Sb}$  (green or light dashed line), and backgrounds from the room and  $^{134}\text{Te}$  build up (gray wide dashed line).

TABLE I: Results for the half-lives of  $^{134}\text{Sb}$  and  $^{134m}\text{Sb}$ . The first uncertainty is statistical, the second is systematic.

Rate	$^{134}\text{Sb}$ $t_{1/2}(\text{s})$	$^{134m}\text{Sb}$ $t_{1/2}(\text{s})$
$\beta$ - $\gamma$ (297 keV)	-	$9.86 \pm 0.06 \pm 0.04$
$\beta$ - $\gamma$ (706 keV)	-	$9.82 \pm 0.09 \pm 0.16$
$\beta$ - $\gamma$ (1279 keV)	-	$9.92 \pm 0.07 \pm 0.07$
$\beta$ - $\gamma$ Average	-	$9.87 \pm 0.04 \pm 0.07$
$\beta$ (Short Cycle)	$0.6744 \pm 0.0034 \pm 0.0019$	$9.87^{\text{a}}$
$\beta$ (Long Cycle)	$0.6744^{\text{a}}$	$9.93 \pm 0.09 \pm 0.07$

<sup>a</sup> Value was fixed in the fit

SATURN/X-Array decay station. Although the  $\beta$  particles emitted following the decay of  $^{134m}\text{Sb}$  are detected with about 1% lower efficiency than those emitted from the decay of  $^{134}\text{Sb}$  because of their lower average energy, this effect was counter balanced by the additional energy deposition from the  $\gamma$  rays emitted in the decay of  $^{134m}\text{Sb}$ . Together, these two effects largely cancel and the  $\beta$ -efficiency ratio for  $^{134m}\text{Sb}$ -to- $^{134}\text{Sb}$  was found to be 1.00(1). The correction for decay prior to measure-

ment accounts for the 30(15)-ms extraction time of the fission products from the CARIBU source to the buncher followed by the 100-ms buncher cycle. These corrections shift the ratio by 8% and after they are applied a value of  $\sigma_h/\sigma_l = 2.03 \pm 0.05$  was obtained.

The isomeric yield ratio can be used to understand the initial angular momentum of the fragments from the fissioning system. This is done using a statistical model of the angular-momentum density distribution of the fragments to determine the imprint the characteristic momentum of the distribution,  $J_{\text{rms}}$ , has on the isomeric yield ratio [2]. Madland and England presented equations for the relation between  $J_{\text{rms}}$  and  $\sigma_h/\sigma_l$  that are only dependent on the spins  $J_g$  and  $J_m$  of the isomeric and ground states, respectively, and ignore the initial excitation energy of the fission fragments and the energy difference between the isomeric and ground state. As  $^{134,134m}\text{Sb}$  has even A and odd  $|J_m - J_g|$ , the relation from Ref. [2] of  $\sigma_h/\sigma_l = \frac{F_4}{(1-F_4)}$  was used, where

$$F_4 = \exp \left[ - (1/J_{\text{rms}}^2) \left( \frac{J_m + J_g + 1}{2} \right) \left( \frac{J_m + J_g + 3}{2} \right) \right].$$

For nuclides with odd A or even  $|J_m - J_g|$ , or both, the relationship between the spins and  $\sigma_h/\sigma_l$  differs, and is described in [2].

TABLE II: This result compared with previous measurements of  $^{252}\text{Cf}$  spontaneous-fission isomeric yield ratios.

Nuclide	$J_g(\hbar)$	$J_m(\hbar)$	$\sigma_h/\sigma_l$	$J_{\text{rms}}(\hbar)^{\text{a}}$
$^{128}\text{Sb}$	$8^-$	$5^+$	$1.1 \pm 0.2^{\text{b}}$	$9.3 \pm 0.6$
			$1.15 \pm 0.35^{\text{e}}$	$9.5^{+1.0}_{-1.2}$
$^{130}\text{Sb}$	$(8^-)$	$(4^+)$	$1.2 \pm 0.2^{\text{b}}$	$9.0 \pm 0.6$
			$0.8 \pm 0.2^{\text{e}}$	$7.7 \pm 0.7$
$^{134}\text{Sb}$	$(0^-)$	$(7^-)$	$2.03 \pm 0.05^{\text{g}}$	$7.07 \pm 0.07^{\text{g}}$
$^{131}\text{Te}$	$\frac{3}{2}^+$	$\frac{11}{2}^-$	$1.8 \pm 0.6^{\text{c}}$	$6.8^{+0.9}_{-1.0}$
$^{133}\text{Te}$	$(\frac{3}{2}^+)$	$(\frac{11}{2}^-)$	$1.2 \pm 0.3^{\text{c}}$	$5.8 \pm 0.5$
$^{132}\text{I}$	$4^+$	$(8^-)$	$1.9 \pm 1.0^{\text{b}}$	$10.8^{+2.1}_{-2.7}$
			$1.11 \pm 0.26^{\text{c}}$	$8.7^{+0.7}_{-0.8}$
$^{134}\text{I}$	$(4)^+$	$(8)^-$	$1.17 \pm 0.30^{\text{b}}$	$8.9^{+0.8}_{-0.9}$
			$1.22 \pm 0.32^{\text{c}}$	$9.0^{+0.9}_{-1.0}$
			$1.68 \pm 0.24^{\text{d}}$	$10.2^{+0.6}_{-0.6}$
$^{136}\text{I}$	$(2^-)$	$(6^-)$	$3.58 \pm 0.40^{\text{b}}$	$10.1 \pm 0.5$
			$3.1 \pm 0.9^{\text{e}}$	$9.5^{+1.1}_{-1.3}$
$^{135}\text{Xe}$	$\frac{3}{2}^+$	$\frac{11}{2}^-$	$1.9 \pm 0.5^{\text{e}}$	$6.9 \pm 0.8$
$^{138}\text{Cs}$	$3^-$	$6^-$	$1.4 \pm 0.4^{\text{f}}$	$7.5^{+0.8}_{-0.9}$

<sup>a</sup> Calculated from the equations of Madland and England [2]

<sup>b</sup> Ref. [6]

<sup>c</sup> Ref. [7]

<sup>d</sup> Ref. [9]

<sup>e</sup> Ref. [10]

<sup>f</sup> Ref. [8]

<sup>g</sup> This work

The characteristic angular momentum obtained from the  $^{134}\text{Sb}$  results is shown in Table II and is at least 1  $\sigma$

lower than the value obtained from previous measurements of  $\sigma_h/\sigma_l$  from other even-A fission products [6, 8–10]. There is a trend identified in proton-induced fission for the value of  $J_{\text{rms}}$  determined from the equations presented by Madland and England to underestimate large and overestimate small  $J_{\text{rms}}$  values when compared to the results of more complex methods that estimate the effects of prompt neutron and  $\gamma$ -ray emission from the primary fission products on the final angular momentum distribution [4, 6]. As the spins for  $^{134,134m}\text{Sb}$  are  $(0^-)$  and  $(7^-)$ , the average spin is lower, resulting in an underestimate when compared to the other measurements with higher spin states. Note that the spin assignments of  $^{134,134m}\text{Sb}$  are tentative and a change to either one would impact the determination of  $J_{\text{rms}}$ . Any assessment of a trend for the spontaneous fission of  $^{252}\text{Cf}$  would require additional high-precision measurements of isomeric yield ratios.

#### IV. CONCLUSIONS

This work demonstrates that by using the mass-separated, high-intensity beams delivered by the CARIBU facility together with the SATURN and X-Array detector systems, it is possible to precisely determine independent yield ratios without relying on absolute  $\gamma$ -ray intensities, even when the half-lives are considerably shorter than 1 s. The results for  $\sigma_h/\sigma_l$  represent the first quantitative measurement for  $^{134}\text{Sb}$  and the most precise measurement of this quantity for any isotope produced in the spontaneous fission of  $^{252}\text{Cf}$ . The value of  $J_{\text{rms}}$  inferred for  $^{252}\text{Cf}$  from this measurement is

lower than values obtained from previous, lower-precision measurements which measured characteristic  $\gamma$  rays for both the isomeric- and ground-state decays in chemically-separated fission-products [6]. In addition, the use of pure beams allowed the quality of the nuclear data on the  $\beta$ -decay half-lives of  $^{134,134m}\text{Sb}$  to be improved significantly. Direct comparisons of isomer yield ratios in spontaneous fission and thermal-neutron-induced fission have previously been limited by the reliance on chemical separation of deposited fission products and yield identification by characteristic  $\gamma$  rays. By applying the measurement approach demonstrated here to other isotopes and other fissioning systems it should be possible to perform more detailed comparisons of the angular momentum distributions of fragments from different fission processes.

#### Acknowledgments

This material is based upon work supported by the National Science Foundation, under Grant Number PHY-1419765 (University of Notre Dame); Department of Energy, National Nuclear Security Administration, under Award Numbers DE-NA0000979 (NSSC), DE-AC52-07NA27344 (LLNL), FOA LAB 17-1763; Office of Nuclear Physics Contract DE-AC02-06CH11357 (ANL), and grants DE-FG02-94ER40848 (UML), DE-AC02-98CH10886 (BNL); NSERC, Canada, under Application No. 216974; Australian Research Council, Grant No. DP130104176 (ANU).

- 
- [1] I. Stetcu, P. Talou, T. Kawano, and M. Jandel, *Phys. Rev. C* **88**, 044603 (2013).
  - [2] D.G. Madland and T.R. England, *Nucl. Sci. and Eng.* **64**, 859 (1977).
  - [3] A. A. Sonzogni, E. A. McCutchan, T. D. Johnson, and P. Dimitriou, *Phys. Rev. Lett.* **116**, 132502 (2016).
  - [4] M. Tanikawa *et al.*, *Z. Phys. A* **347**, 53 (1993).
  - [5] S. Goto *et al.*, *J. Radioanal. Nucl. Chem.* **239**, 109 (1999).
  - [6] H. Kudo, R. Saito, and M. Oda, *Radiochimica Acta* **69**, 145 (1995).
  - [7] H. N. Erten *et al.*, *J. Inorg. Nucl. Chem.* **40**, 183 (1978).
  - [8] T. Datta *et al.*, *Z. Phys. A* **324**, 81 (1986).
  - [9] H. Naik *et al.*, *Z. Phys. A* **331**, 335 (1988).
  - [10] H. Naik *et al.*, *Nucl. Phys. A* **587**, 273 (1995).
  - [11] H. Naik *et al.*, *Nucl. Phys. A* **648**, 45 (1999).
  - [12] J. Shergur *et al.*, *Phys. Rev. C* **71**, 064321 (2005).
  - [13] A. Kerek, G. B. Holm, S. Borg, and L.-E. de Geer, *Nuclear Physics A* **195**, 177 (1972).
  - [14] A. Kankainen *et al.*, *Phys. Rev. C* **87**, 024307 (2013).
  - [15] A. A. Sonzogni, *Nucl. Data Sheets* **103**, 1 (2004).
  - [16] K. Siegl *et al.*, *Phys. Rev. C* **97**, 035504 (2018).
  - [17] G. Savard *et al.*, *Nucl. Instrum. Methods Phys. Res., Sect. B* **266**, 4086 (2008).
  - [18] G. Savard *et al.*, *Nucl. Instrum. Methods Phys. Res., Sect. B* **376**, 246 (2016).
  - [19] C.N. Davids and D. Peterson, *Nucl. Instrum. Methods Phys. Res., Sect. B* **266**, 4449 (2008).
  - [20] A.J. Mitchell *et al.*, *Nucl. Instrum. Methods Phys. Res., Sect. A* **763**, 232 (2014).
  - [21] G. Rudstam, K. Aleklett, and L. Sihver, *Atomic Data and Nuclear Data Tables* **53**, 1 (1993).
  - [22] B. Grapengiesser, E. Lund, G. Rudstam, *J. Inorg. Nucl. Chem.* **36**, 2409 (1974).
  - [23] E. Lund, G. Rudstam, *Phys. Rev. C* **13**, 1544 (1976).
  - [24] A. A. Delucchi *et al.*, *Phys. Rev.* **173**, 1159 (1968).
  - [25] B. Fogelberg *et al.*, *Phys. Rev. C* **41**, R1890(R) (1990).